

Upscaling Elastic Properties: A Case Study

Mehdi Khajeh, Jeff Boisvert and Rick Chalaturnyk

Use of coupled geomechanical flow simulation is important for characterizing SAGD processes because a) rock deformation during extraction affects production performance and b) cap rock integrity is important for SAGD performance. These simulations require modeling of rock mechanical properties. Geostatistical techniques could be used to capture small scale variation of rock mechanical properties; however, due to the high computational time required for coupled simulation process, these fine scale geological models are not suitable choices for simulation. Upscaling techniques are introduced to upscale these geological models to appropriate simulation scales. Reproducing fine scale geomechanical responses, such as volumetric strain, within an acceptable range of errors is a key factor which should be considered when checking/validating upscaling accuracy. A new numerical upscaling technique has been proposed in paper 118 (this report). Here, the accuracy of the proposed upscaling technique is compared to power law averaging. For that purpose, one MEM realization has been selected to implement the coupled geomechanical flow simulation of a SAGD process. Volumetric strain of the fine scale geological model is considered as the base geomechanical response of the media to which the upscaling techniques are compared. The proposed numerical upscaling technique and power law averaging techniques provide various upscaled elastic property models. The volumetric strain of these upscaled models are compared to the base geomechanical response and show that the proposed numerical upscaling technique performs well.

Introduction

Subsurface formations typically display high degrees of variability over fine scales and geostatistical techniques are used to characterize these fine scale variations. The McMurray formation in Alberta-Canada is a stress dependent reservoir. In SAGD, high pressure/high temperature steam injection cause non-negligible variations in in-situ stresses and deformation which effect reservoir performance. In addition to conventional flow simulation, consideration of the stress field and deformation effects is important.

The change in stress state affects petrophysical properties such as porosity and permeability and can have a large impact on reservoir productivity (Merle et al., 1976; Heffer et al., 1994). Coupled geomechanical flow simulation should be considered as a part of SAGD performance prediction. A Mechanical Earth Model (MEM) is a heterogeneous geological model containing models of petrophysical properties and geomechanical properties which are required for coupled geomechanical flow simulation (see paper 114 in this report). Upscaling is required as the computational requirements of coupled geomechanical flow simulation are not feasible at the point scale typical of sequential Gaussian simulations.

Due to lack of data for defining fine scale MEM realizations, homogeneous (layer cake) models are often considered for elastic properties in geomechanical simulations. In this approach, rock mechanical properties are usually defined directly from core sample experiment results without consideration of the facies distribution within the reservoir. This approach may lead to erroneous modeling as the geomechanical behavior of sand and shale are quite different. Accounting for the fine scale heterogeneity of equivalent properties from analytical or numerical upscaling methods will result in a better definition of elastic properties. This increases the accuracy of large scale geomechanical simulations resulting in better flow response prediction.

The proposed numerical upscaling technique is detailed in papers 118 and 119 in this report. This work considers applying the proposed upscaling methodology on one of the MEM realizations created as per paper 114 in this report. Volumetric strain is considered as the geomechanical response of interest. The response of the fine scale simulation is considered as the true response of the geological model and is compared with the volumetric strain maps obtained from different upscaling techniques, i.e. the proposed numerical upscaling and power law averaging.

In addition to elastic properties, petrophysical properties, i.e. porosity and absolute permeability, are also required at the upscaled block size; however, the focus here is to check the accuracy of the proposed numerical upscaling technique for geomechanical variables so consistent upscaling approaches for petrophysical properties have been considered in all cases. Arithmetic averaging for porosity and numerical local upscaling are used for upscaling of porosity and permeability respectively.

Porosity/Permeability upscaling

Porosity on the coarse scale is computed such that pore volume is conserved between the fine and coarse scales:

$$\phi^* = \frac{1}{V_b} \int_{V_b} \phi(y) dV \quad (1)$$

where,

Φ^* : Coarse scale permeability

V_b : coarse scale volume

$\Phi(y)$: fine scale permeability

For permeability upscaling, a local upscaling approach is used. Local upscaling (Pickup et al., 1994; Durlofsky, 1991; Durlofsky, 2005 to name a few) is the solution of the governing fine scale pressure equations for flow with an assumed boundary condition for the fine grid blocks that are contained in a single coarse cell (Figure 1a). The cells surrounding the coarse block of interest are ignored. Different boundary conditions are often considered with constant pressure and no flow boundaries (Figures 1b and 1c). Effective permeability in different directions is obtained. From the configurations shown in Figure 1b and 1c, effective permeability in the horizontal and vertical directions (i.e. K_x^* and K_y^*) can be calculated respectively. "FLOWSIM" (Deutsch, 1998) has been used for this purpose.

Power Law Averaging

In addition to numerical upscaling, arithmetic, harmonic and geometric averaging (Equations 2, 3 and 4 respectively) are used to make a comparison between proposed numerical upscaling approach and analytical averaging techniques.

$$A_{arithmetic}^* = \left(\sum_{i=1}^n A_i h_i \right) / \sum_{i=1}^n A_i \quad \text{Eq (2)}$$

$$A_{harmonic}^* = \sum_{i=1}^n L_i / \sum_{i=1}^n \left(\frac{L}{A} \right)_i \quad \text{Eq (3)}$$

$$A_{geometric}^* = \exp \frac{1}{n} \sum_{i=1}^n \log A_i \quad \text{Eq (4)}$$

A generalization of these averaging techniques is Power Law averaging, developed by Deutsch (1989):

$$k_w = \left(\frac{1}{n} \sum_{i=1}^n k_i^w \right)^{1/w} \quad \text{Eq (5)}$$

Numerical Upscaling of Elastic Properties

A detailed description of the numerical upscaling is in paper 118 in this report. Figure 2 shows the conceptual framework used. When considering heterogeneous media (Figure 2a) the loading process would result in complex deformation (Figure 2b). After upscaling this system to a single block, the goal is to reproduce the average fine scale deformation in the coarse scale block (Figure 2c). The coarse upscaled property (yellow block in Figure 2c) is the value that results in the average displacement had the fine scale model been deformed. Considering a local upscaling framework with Hook's Law as the governing equation results in the calculation of equivalent elastic properties of the upscaled cell.

Model Description

To decrease boundary effects, the dimensions of a model considered for geomechanical analyses is usually 3 to 4 times larger than dimensions of the model considered for flow analysis. In addition to the common reservoir section between the two simulators, i.e. flow and geomechanical simulator, additional depth above and below the reservoir (overburden and underburden) and sideburden are considered in the geomechanical model (Figure 3). As the reservoir is the only section which is considered for coupled geomechanical-flow analysis, a coarser grid was considered for the regions surrounding the reservoir.

Fixed horizontal displacement for all sides of the model and fixed vertical displacements at the bottom of the model are considered. In-situ stress configuration (i.e. magnitudes and directions) has a significant impact on the geomechanical response and affects the optimization of injection pressure to prevent cap-rock instability, the maximum dilatancy of the reservoir, and the selection of drilling direction to maximize SAGD performance. The magnitudes selected for minimum and maximum horizontal stresses, pore pressure and vertical stress are based on Collins (2002) and are given in Table 1.

Linear elastic deformation is considered for all model regions (Figure 3). Table 2 lists the properties considered for over, side and underburden. MEM Realization (Figure 4) is considered. The procedure for generating this realization is discussed in paper 114 in this report. Additional rock mechanical properties are required for flow simulation and are summarized in Table 3. Parameters in Table 2 and Table 3 are selected based on previous studies (Chalaturnyk, 1996; Li, 2006).

Error Analysis

The same process as applied for papers 118 and 119 are used here for error analysis. Considering volumetric strain as geomechanical response and following Equation:

$$[\%]e = \frac{\sum_r \left| 1 - \frac{\bar{e}_{v_r}}{e_{v_r}} \right|}{n_r} * 100 \quad \text{Eq (6)}$$

where:

\bar{e}_{v_r} is the average volumetric strain of the fine scale cells in the r^{th} upscaled block, Equation 25.

e_{v_r} is the volumetric strain in the r^{th} upscaled block.

n_r is the number of blocks in the upscaled model.

and

$$\bar{e}_{v_r} = \frac{\sum_i e_{v_i}}{n_i} * 100 \quad \text{Eq (7)}$$

where,

e_{v_i} is the volumetric strain in the i^{th} fine scale cell within the upscaled block.

Ten upscaling ratios (number of fine scale cells in each upscaled block) are considered to assess the accuracy of upscaling methodology in this work; horizontal ratios of 1:1, 5:1, 10:1, 20:1, 50:1, and vertical ratio of 2:1 and 8:1.

Results

In Figures 5 and 6 the results of upscaling of Young Modulus with arithmetic and the proposed numerical (x_m) upscaling techniques are shown for vertical upscaling ratios of 2:1 and 8:1 respectively. Similar results are obtained for two other analytical techniques, i.e. geometric and harmonic techniques.

Averaging in the vertical direction has a larger effect on upscaling because of the shorter vertical variogram range typical of the McMurray formation. The visual difference in the upscaled results between averaging and the proposed numerical technique (Figures 5 and 6) appear minimal; however, the resulting volumetric strain error is apparent. Using the error definition (Equation 6) the effect of different upscaling processes on volumetric strain is shown (Figure 7). The proposed numerical averaging technique is superior for all vertical and horizontal ratios considered. Uncertainty in this response will be determined by processing multiple realizations.

Conclusion

The proposed numerical upscaling technique is tested on an MEM realization for a SAGD process. Porosity is effected by geomechanical processes during SAGD. Change in porosity is known to be linked to volumetric strain (Tortike and Farouq Ali, 1993). Incorporating volumetric strain in SAGD simulation is vital as it has a large effect on accurate estimation of the change in porosity (and other reservoir parameters) and effects the prediction of reservoir performance, i.e. cumulative oil production. The proposed numerical upscaling technique shows promise for better assessing the upscaled response of reservoirs that are stress dependent.

References

Merle HA, Kentie CJP, Van Opstal GHC, Schneider GMG. The Bachaquero study- a composite analysis of the behavior of a compaction drive/solution gas drive reservoir. SPE Journal of Petroleum Technology 1976; Trans., AIME, 261: 1107–1115.

Heffer KJ, Last NC, Koutsabeloulis NC, Chan HCM, Gutierrez M, Makurat A. The influence of natural fractures, faults and earth stresses on reservoir performance- geomechanical analysis by numerical modelling. North Sea Oil and Gas Reservoirs 1994; 3:201–211.

Durlofsky, L. J. 1991. Numerical calculation of equivalent grid block permeability tensors for heterogeneous porous media. Water Resources Research. 27: 5,669–5,708

Pickup, G.E., P.S. Ringrose, J.L. Jensen and K.S. Sorbie .1994. Permeability tensors for sedimentary structures. Mathematical Geology. 26: 2–227,2–250

Durlofsky, L.J. 2005. Upscaling and gridding of fine scale geological models for flow simulation. Presented at 8th international forum of reservoir simulation, Stresa, Italy.

Deutsch, C. V. and A. G Journel. 1998. GSLIB: Geostatistical Software Library and User’s Guide. Second edition, Oxford, New York.

Deutsch, C.V. 1989. Calculating Effective Absolute Permeability in Sandstone/Shale Sequences. SPE Formation Evaluation. 4: 3,343–3,348.

Collins, P.M. 2002. Injection Pressures for Geomechanical Enhancement of Recovery Process in the Athabasca Oil Sands. SPE 79028 presented at SPE International Thermal Operations and Heavy Oil Symposium and International Horizontal Well Technology Conference, 4-7 November, Calgary, Alberta, doi: 10.2118/79028-MS

Chalaturnyk, R. 1996. Geomechanics of the Steam-Assisted Gravity Drainage Process in Heavy Oil Reservoirs. PhD dissertation, University of Alberta, Edmonton, Canada.

Li, P., 2006. Numerical simulation of the SAGD process coupled with geomechanical behavior. PhD dissertation, University of Alberta, Edmonton, Canada.

Tortike, W.S., 1991. Numerical Simulation of Thermal Multiphase Fluid Flow in an Elastoplastic Deforming Oil Reservoir. Ph.D dissertation, School of Mining and Petroleum Engineering, Department of Civil and Environmental Engineering, University of Alberta.

Tables

Table 1. Initial stress, Pore Pressure and Temperature for the Model Under Study [After Collins (2002)]

Parameter	Value
Reservoir Depth	470 meter
σ_h / σ_v	1
σ_H / σ_v	1.5
Initial reservoir pressure	2.7 MPa
Initial reservoir temperature	12 °C

Table 2. Properties Considered for Over, Under and Side Burdens for the Model Under Study

Zone	Parameter	Value
Overburden	Bulk Density (kg/m ³)	2200
	Bulk Modulus (MPa)	208
	Shear Modulus (MPa)	96.2
	Linear Thermal Expansion coefficient (°K ⁻¹)	2×10 ⁻⁵
Sideburden	Bulk Density (kg/m ³)	2200
	Bulk Modulus (MPa)	620
	Shear Modulus (MPa)	286
	Linear Thermal Expansion coefficient (°K ⁻¹)	2×10 ⁻⁵
Underburden	Bulk Density (kg/m ³)	2200
	Bulk Modulus (MPa)	4167
	Shear Modulus (MPa)	1923
	Linear Thermal Expansion coefficient (°K ⁻¹)	2×10 ⁻⁵

Table 3. Rock Parameters Used in Flow Simulator

Parameter	Value
Rock Compressibility (1/kPa)	5×10 ⁻⁶
Rock Expansion Coefficient (°C ⁻¹)	3.84×10 ⁻⁵
Rock Heat Capacity (kJ/kg°K)	1865
Rock Thermal Conductivity (W/m°K)	1.736

Figures

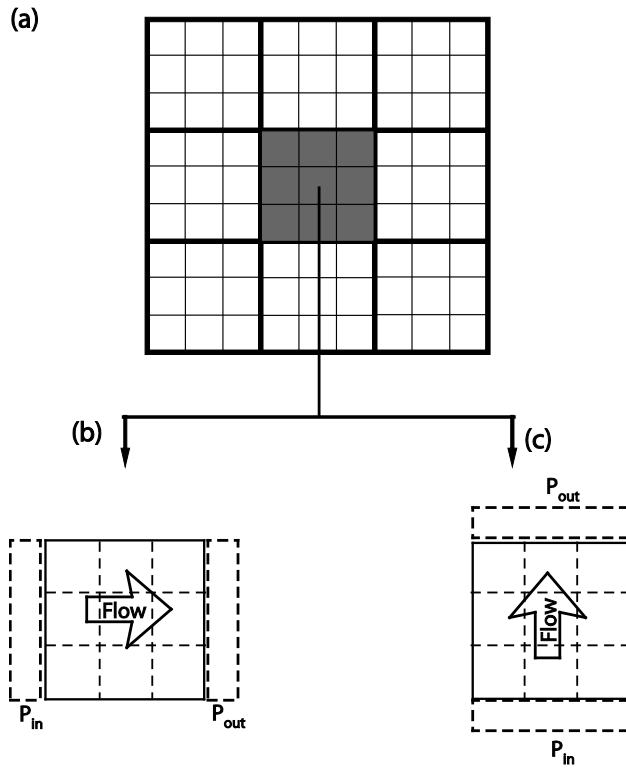


Figure 1. Schematic of Pure Local Upscaling.

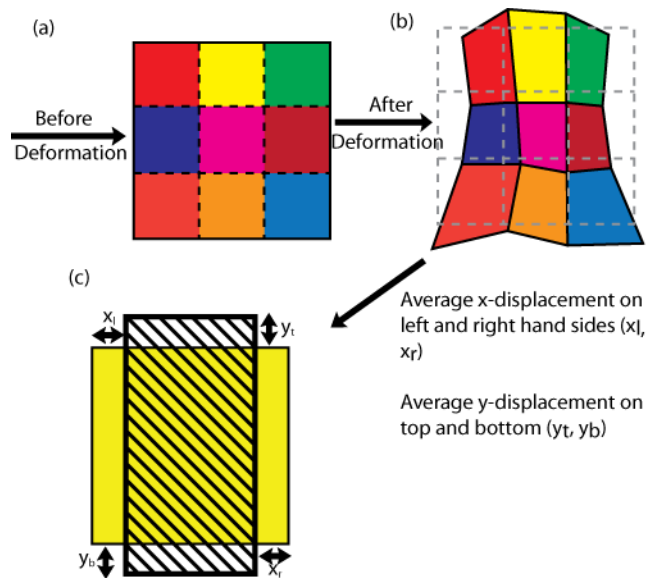


Figure 2. Conceptual Framework for Numerical Upscaling of Elastic Properties.

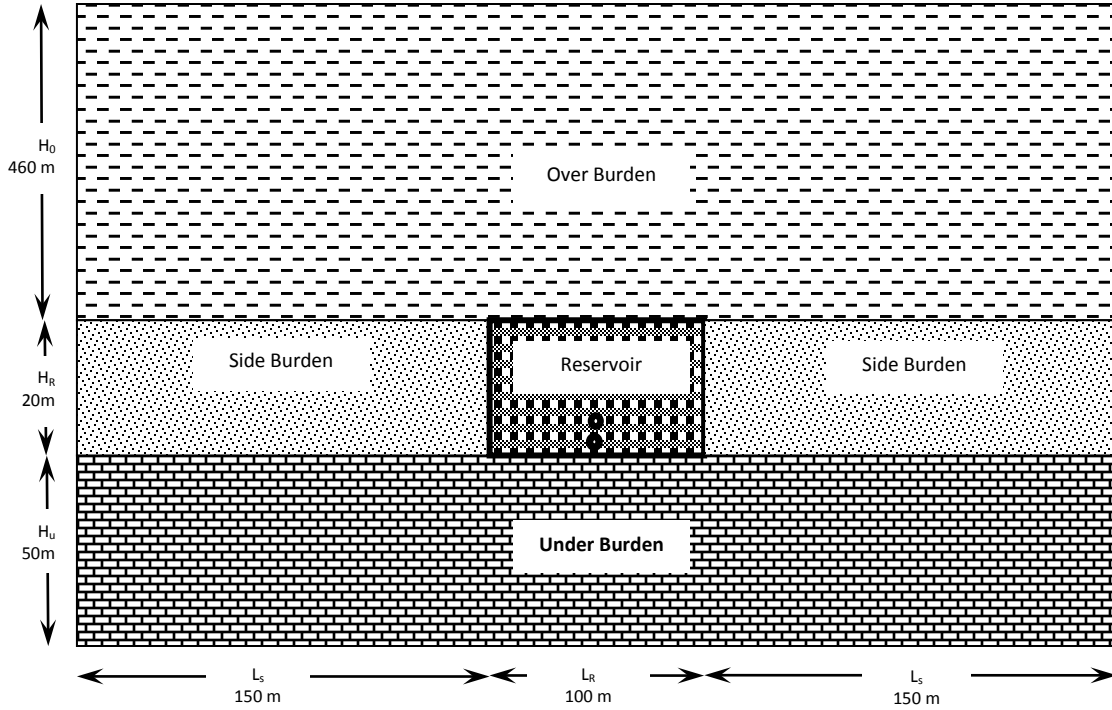


Figure 3. Model description and dimensions used for this study

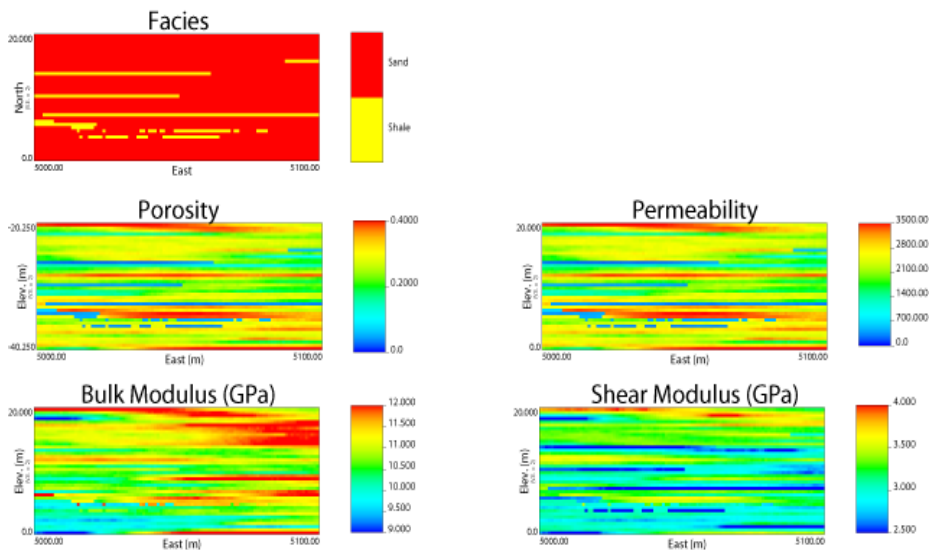


Figure 4. MEM Realization Considered for Reservoir Section shown in Figure 3.

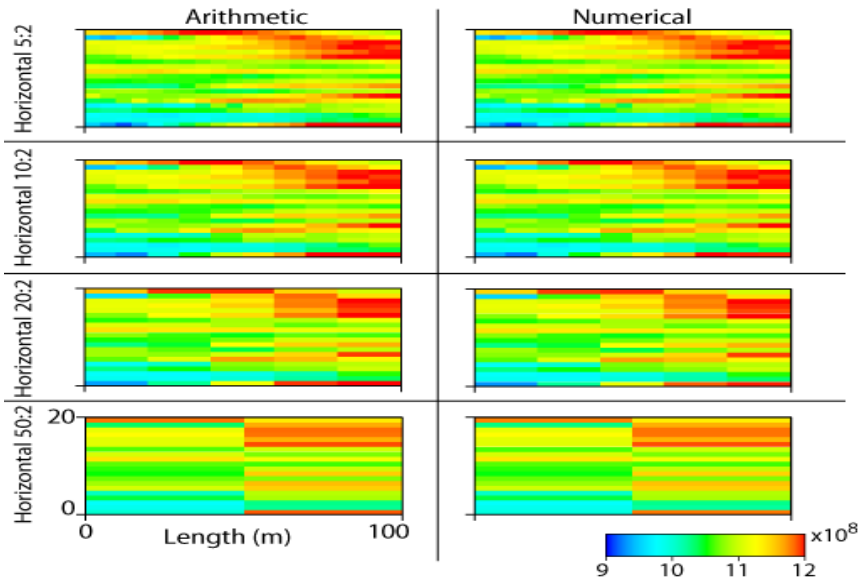


Figure 5. Young modulus for different horizontal upscaling ratios, vertical upscaling ratio is constant at 2:1.

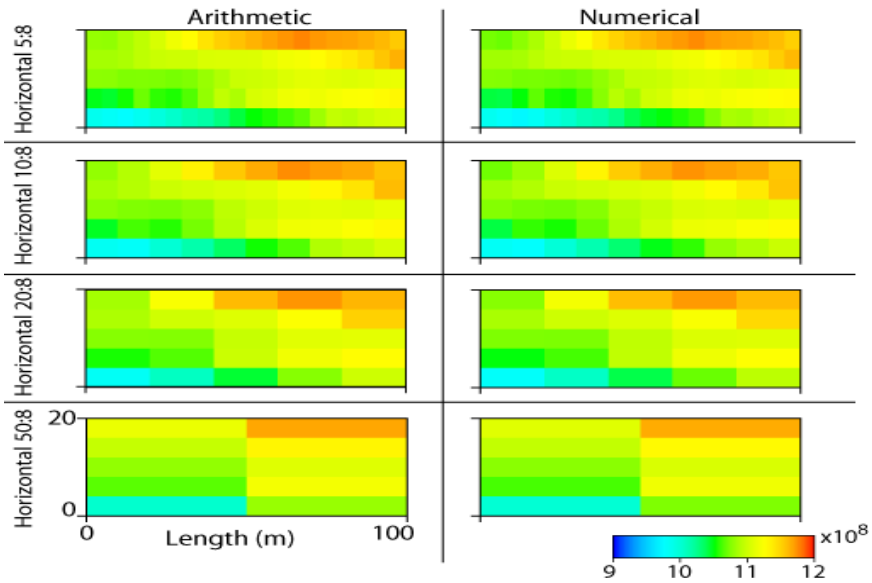


Figure 6. Young modulus for different horizontal upscaling ratios, vertical upscaling ratio is constant at 8:1.

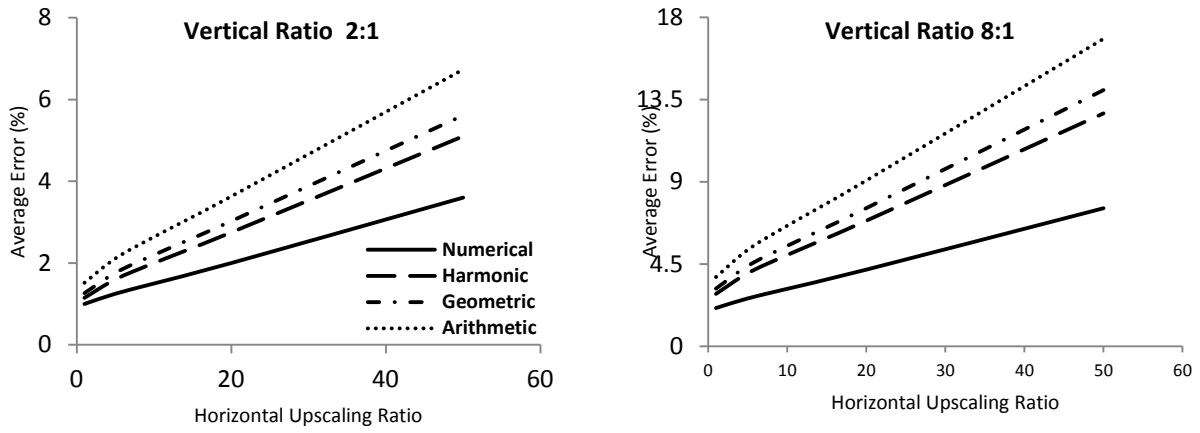


Figure 7. Average error for considered horizontal and vertical upscaling ratios.